Analysis of Field Propagation inside A Waveguide Diplexer using Cavity Model Analysis

Ashmi Chakraborty[1]* and Santanu Dwari[2]

[1] *Department of Electronics and Communication Engineering, Asansol Engineering College, Asansol, West Bengal 713305, India*
[2] *Department of Electronics Engineering, Indian Institute of Technology (ISM), Dhanbad, Jharkhand 826004, India*
**ashmi.chakraborty@gmail.com*

Abstract. This paper presents a numerical analysis of field propagation inside a waveguide diplexer network. To do the analysis the diplexer network has been modeled using multiple cavities and then solved using a method of moments. Field propagation inside the network has been demonstrated in terms of aperture field distributions at various transverse planes of the network at the two-channel frequencies and a stopband frequency. To validate the numerical analysis, the frequency responses of the diplexer have been compared with literature available data.

Keywords: Aperture field distribution, cavity modeling, method of moments, Galerkin's method

1. Introduction

Waveguide diplexer networks are widely used in high-power multi-service multi-band communication systems, like satellite communication systems, to split a broad frequency band into two narrower bands or combine two narrow frequency bands into one broad frequency band. This prompted the microwave researcher to analyze, design and develop waveguide diplexers for several decades. Subsequently, a large number of diplexer networks were developed using different filter and combiner geometry [1-15]. Several techniques were used to design and analyze these diplexers, which include, the matrix method [1], Eigenmode analysis [2], modal S-matrix method [3], field theory method [4], a combination of the standard mode-matching technique with the coupled-integral-equations technique [5], full wave optimization [6], generalized scattering matrix [7], dimensional synthesis using electromagnetic simulator [8], mode matching technique [9], generalized admittance matrix [10], and computer-aided design [11-15]. The main objective of these works was to provide design equations/steps to design the diplexer and subsequently present a diplexer circuit based on these equations/steps. However, none of them exactly describes how the wave propagates inside the network. Alternatively, how the wave with a desired frequency is diverted to the designated output port and how the wave with an undesired frequency is prevented from reaching any output ports.

This paper presents a field-theoretic approach [16,17] that can be used to analyze the field propagation inside a diplexer network and understand the working principle of the network. Since a large number of diplexer networks are already available in open literature with excellent network characteristics, it felt useless to design another diplexer network. Instead, the diplexer network, presented in [10], has been considered as an example. The analysis clearly describes the propagation of fields inside the network at different pass band and stop band frequencies using the aperture field distributions on various transverse planes of the network. The analysis, thus, will be helpful for the future design of more advanced diplexer networks in terms of compactness, frequency suppression, and channel isolation.

2. Cavity model analysis

The 3D cut-plane view of the H-plane T-Junction diplexer network under consideration is shown in Figure 1 and its cavity modeling is shown in Figure 2. It consists of three waveguide regions (W_1-W_3), twenty cavity regions (C_1-C_{20}), and twenty-two apertures (A_1-A_{22}) between them. In the structure port 1 (W_1) corresponds to the common input port and ports 2 and 3 (W_2 and W_3) correspond to the channel output ports. The electric fields on the apertures between different regions are unknown and can be replaced by unknown fictitious magnetic current densities (M_1-M_{22}) existing on electric conductors with the help of the equivalence principle. This converts the different waveguide sections between the apertures into equivalent cavities. In Figure 2, apertures A_1-A_{12} are on the *xy*-plane whereas apertures A_{13}-A_{22} are on the *yz*-plane. Therefore, the tangential components of M_1-M_{12} are x and y whereas the tangential components of M_{13}-M_{22} are y and z, respectively. The unknown magnetic currents on the apertures can be assumed as a weighted piecewise triangular basis function.

The magnetic fields present in a given region of the network (waveguide/cavity) can be of the following types: (1) source or incident field and (2) scattered field due to the magnetic currents at the apertures. If the scattered field is in the waveguide region then it is called a 'waveguide scattered field' whereas if the scattered field is in the cavity region then it is called the 'cavity scattered field'. The scattered field in the waveguide region can be derived using the modal expansion method [16-18] whereas the scattered field in the cavity regions can be derived using the Greens function approach [16, 17, 19]. The source field is the dominant TE_{10} mode and can be present in the input waveguide only (in this case in the region W_1). The net magnetic field in a given region can be found by using the superposition principle.

Applying the continuity condition of tangential magnetic fields, the boundary equations on the different apertures of the

DOI: http://dx.doi.org/10.32452/IJAMT.2022.296300

network can be derived. The boundary equation will be in terms of unknown magnetic currents and can be solved using Galerkin's specialization of the method of moments [16, 17, 20]. This will provide the fields at different apertures and S-parameters of the network.

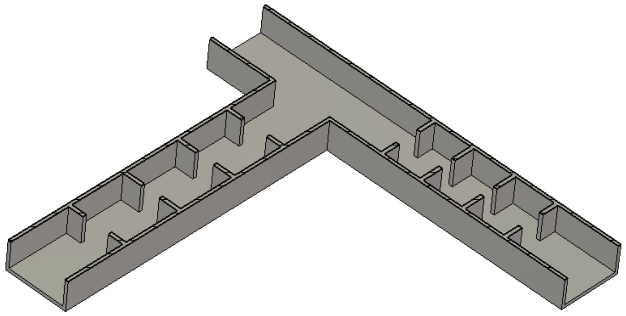

Fig.1. 3D cut plane view of the H-plane T-Junction diplexer.

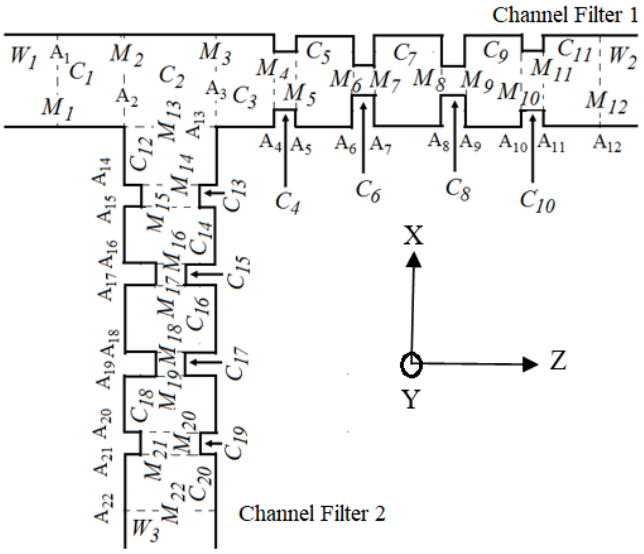

Fig.2. Cavity modeling of the H-plane T-Junction diplexer using the twenty-cavity approach (top view) with magnetic current at the apertures.

3. Results and discussion

The electric field distributions on the different apertures of the diplexer have been plotted in Figure 3 at 8.84 GHz (pass band frequency of channel filter 2), in Figure 4 at 10 GHz (stop band frequency for both channel filters), and Figure 5 at 10.94 GHz (pass band frequency of channel filter 1), respectively. The electric field distributions at the input of channel filter 1 (aperture 3) and channel filter 2 (aperture 13) at 8.84 GHz are shown in Figure 3 (a) and Figure 3 (b), respectively. The figures reveal that the electric field is more concentrated in aperture 13 than in aperture 3, signifying the branching of power towards channel filter 2. The electric field distributions at the output of channel filter 1 (apertures 12) and channel filter 2 (apertures 22) are plotted in Figure 3 (c) and Figure 3 (d), respectively. The figures reveal that a signal of frequency 8.84 GHz will be channeled to channel filter 2 and will exit from it whereas no output will be obtained from channel filter 1.

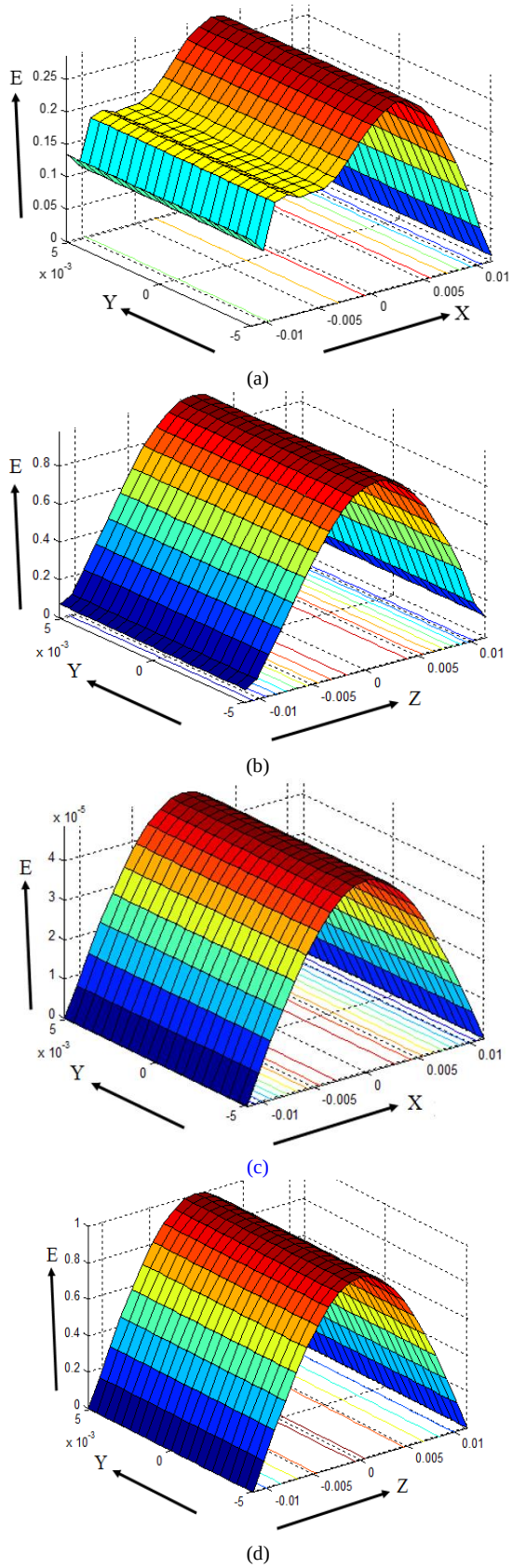

Fig.3. Electric field distributions (in V/m) on (a) aperture 3, (b) aperture 13, (c) aperture 12, and (d) aperture 22 of the diplexer at 8.84 GHz. X/Y/Z represents the corresponding side of the aperture in m.

DOI: http://dx.doi.org/10.32452/IJAMT.2022.296300

Figure 4 (a) reveals that only a part of the incident electric field is coupled to the input port of the diplexer at 10 GHz (the incident field is of unit amplitude). The coupled electric field is then branched into channel filters 1 (Figure 4 (b)) and 2 (Figure 4 (c)) and continuously decays in amplitude in channel filter 1 and in channel filter 2. Finally, a negligible field exists at the output apertures (Figure 4 (d) and Figure 4(e)). This represents the stopband characteristics of the diplexer at 10 GHz.

Propagation of the electric field in the diplexer at 10.94 GHz is shown in Figure 5. Figure 5 (a) and Figure 5 (b) reveal that the electric field is more concentrated in aperture 3 than in aperture 13, signifying the branching of power towards channel filter 1. The electric field distributions at the output of channel filter 1 (apertures 12) and channel filter 2 (apertures 22) are plotted in Figure 5 (c) and Figure 5 (d), respectively. The figures reveal that a signal of frequency 10.94 GHz will be channeled to channel filter 1 and will exit from it whereas no output will be obtained from channel filter 2.

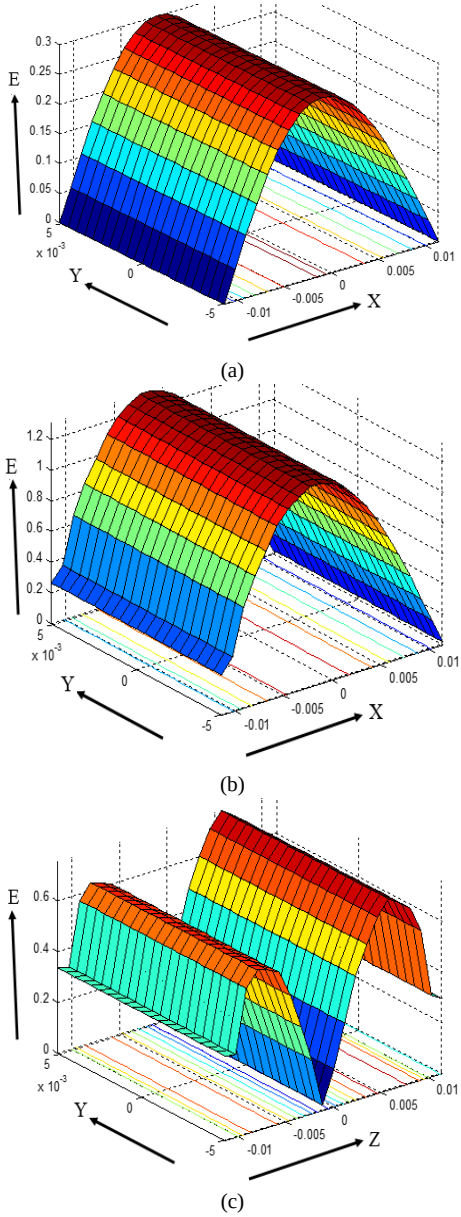

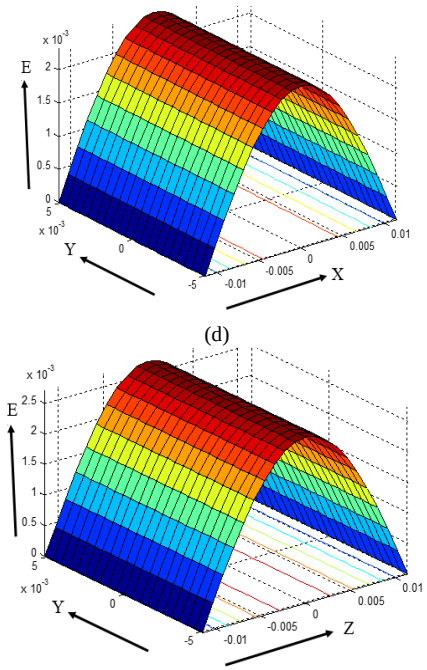

Fig.4.: Electric field distributions (in V/m) on (a) aperture 1, (b) aperture 3, (c) aperture 13, (d) aperture 12, and (e) aperture 22 of the diplexer at 10 GHz. X/Y/Z represents the corresponding side of the aperture in m.

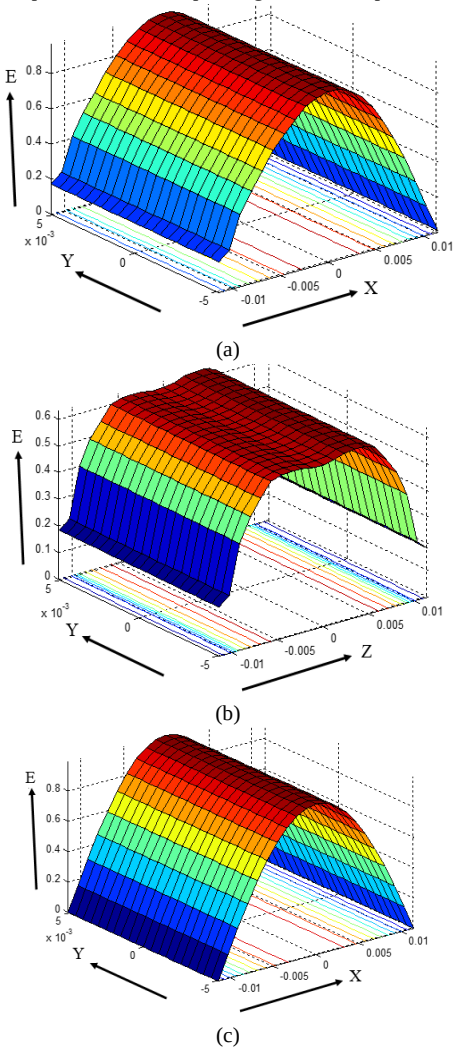

DOI: http://dx.doi.org/10.32452/IJAMT.2022.296300

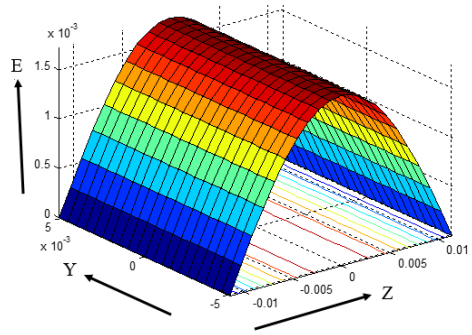

(d)

Fig.5. Electric field distributions (in V/m) on (a) aperture 3, (b) aperture 13, (c) aperture 12, and (d) aperture 22 of the diplexer at 10.94 GHz. X/Y/Z represents the corresponding side of the aperture in m.

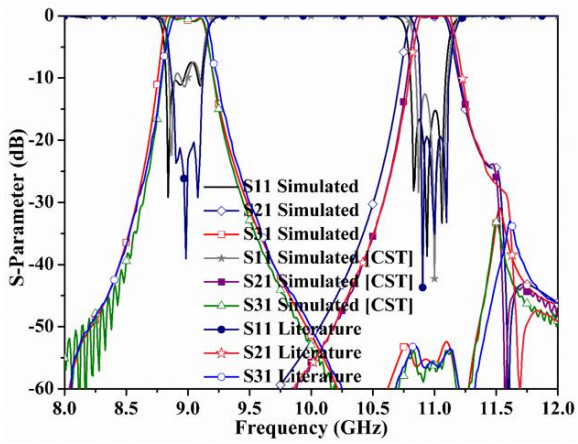

Fig.6. Comparison of the frequency response obtained using the proposed method with the frequency response presented in the literature [10].

The analysis of the aperture field distributions in Figure 3 to Figure 5 reveals two pass bands centered around 8.84 GHz and 10.94 GHz and a stop band centered around 10 GHz. The complete frequency response of the diplexer, from 8-12 GHz, is shown in Figure 6 and compared with the literature available data [10]. The figure reveals a close agreement between the data obtained using the proposed method and from the literature. Figure 4(d) and Figure 4(e) reveal that at 10 GHz the magnitudes of the electric field at the outputs of the channel filter 1 (aperture 12) and channel filter 2 (aperture 22) are almost the same and around 2.5*10-3 V/m, which are in accordance to Figure 6 that reveals that S21 and S31 are almost same and around -50 to -55 dB. Figure 5 (d) also shows that the magnitude of the electric field at the output of channel filter 2 (aperture 22) at 10.94 GHz is around 2*10-3 V/m. Therefore, it is expected that at 10.94 GHz, S_{31} should also be around -50 to -55 dB; which is in accordance with Figure 6. On the contrary, Figure 3 (c) shows that the magnitude of the electric field at the output of channel filter 1 (aperture 12) at 8.84 GHz is around 5*10-4 V/m, which is quite smaller compared to the others, indicating better isolation. The same has been reflected in Figure 6, which shows that the S21 at 8.84 GHz is well below -60 dB and hence not reflected in the figure. Similar other observations and agreements between Figure 6 and Figure 3 to 5 can be obtained by comparing the magnitudes of the S-parameters in Figure 6 and corresponding magnitudes of the electric field at the input/output ports of the diplexer in Figure 3 to 5 at different frequencies These agreements, in turn, verify the proposed numerical analysis of the structure. The slight discrepancies between the results are because all the optimized dimensions of the diplexer are not provided in the literature and these dimensions are assumed to be equal to the initial dimensions.

4. Conclusions

This paper presents a numerical analysis of an H-plane T-Junction diplexer network and explains its field propagation. The analysis reveals that the channel filters do not abruptly reject the stop band frequencies, instead, they gradually reject them. For a stop band frequency, rejection starts at the input port of the diplexer. The TE_{10} mode type field distributions on the apertures, except on apertures 3 and 13, imply that the generated higher order modes at the steps are not strong enough. This is because the TE_{10} mode does not depend on the y-component. Moreover, the irises separating the cavities are inductive and do not excite the y-dependence of the fields. The analysis of the diplexer has been carried out by modeling the structure using twenty cavities and three waveguide sections and using Galerkin's specialization of the method of moments. The reasonable agreement between the obtained, CST Microwave Studio simulation and the literature available data implies that the proposed technique is capable of analyzing a complicated structure, like this. The proposed technique is general and can be used to analyze the field propagation in any rectangular waveguide-based diplexer (and other) networks.

Acknowledgment

The authors will like to thank Dr. Sushrut Das, Associate Professor, Department of Electronics Engineering, Indian Institute of Technology (Indian School of Mines) Dhanbad for his suggestions during this work.

References

[1] N. Nakajima, and I. Ohtomo, 80-GHz-Band Low-Loss Ring-Type Channel Diplexer Using a Semicircular Electric Mode, *IEEE Transactions on Microwave Theory and Techniques*, vol. 24, no. 11, pp. 831- 836, 1976.

[2] F. Arndt, J. Bornemann, D. Grauerholz, D. Fasold, and N. Schroeder, *Waveguide E-Plane Integrated-Circuit Diplexer*, *Electronics Letters*, vol. 21 no. 14, pp. 615-617, 1985.

[3] F. Arndt, J. Dittloff, U. Papziner, D. Fasold, N. Nathrath, and H. Wolf, Rigorous Field Theory Design of Compact and Lightweight Broadband Diplexers for Satellite Communication Systems, *19th European Microwave Conference*, pp. 1214-219, 1989.

[4] J. Bomemann, Design of Millimeter-Wave Diplexers with Optimized H-Plane Transformer Sections, *Canadian Journal of Electrical and Computer Engg*, vol. 15 no. 1, pp. 5-8, 1990.

[5] S. Amari, J. Bornemann, W. Menzel, and F. Alessandri, Diplexer Design using Pre-Synthesized Waveguide Filters with Strongly Dispersive Inverters, *IEEE MTTs International Microwave Symposium*, pp. 1627-1630, 2001.

[6] T. Shen, K. A. Zaki, and T. G. Dolan, Rectangular Waveguide Diplexers with a Circular Waveguide Common Port, *IEEE Transactions on Microwave Theory and Techniques.*, vol. 51, no. 2, PP. 578-582, 2003.

[7] C. Tomassoni, L. Marcaccioli, M. Dionigi, M. Mongiardo, R. Vincenti Gatti and R. Sorrentino, CAD of Folded Filters and

Diplexers by the Generalized Scattering Matrix of the Single Step Discontinuity, *IEEE MTTs International Microwave Symposium*, pp. 1843-1846, 2004.

[8] F. M. Vanin, D. Schmitt, and R. Levy, Dimensional Synthesis for Wide-Band Waveguide Filters and Diplexers, *Transactions on Microwave Theory and Techniques*, vol. 52, no. 11, pp. 2488-2495, 2004.

[9] E. Ofli, Member, R. Vahldieck, and S. Amari, Novel E-Plane Filters and Diplexers with Elliptic Response for Millimeter-Wave Applications, *IEEE Transactions on Microwave Theory and Techniques*, vol. 53, no. 3, pp. 843-851, 2005.

[10] Y. Tao, Z. Shen, Closed-form Expression for the Equivalent Circuit Model of H-Plane Waveguide T-Junctions, *IET Microwave and Antenna Propagation.*, vol. 4, issue 12, pp. 2008-2013, 2008.

[11] X. Shang, Y. Wang, W. Xia, and M. J. Lancaster, Novel Multiplexer Topologies Based on All-Resonator Structures, *IEEE Transactions on Microwave Theory and Techniques*, vol.61, no.11, pp. 3438-3845, 2013.

[12] W. Xia, X. Shang, and M. J. Lancaster, All-Resonator Based Waveguide Duplexer with Cross-Coupling, *Electronics Letters*, vol. 50, no. 25, pp. 1948 – 1950, December 2014.

[13] J. R. Aitken, J. Hong, Design of Millimeter Wave Diplexers with relaxed fabrication Tolerance, *IET Microwave, Antennas and propagation*, vol. 9, issue 8, pp. 802 - 807, 2015.

[14] L. Zhu, R. R. Mansour, and M. Yu, Compact Waveguide Dual-Band Filters and Diplexers, *IEEE Transactions on Microwave Theory and Techniques*, vol. 65, no. 5, pp. 1525 – 1533, May 2017.

[15] F. Teberio, I. Arregui, P. Soto, M. A. G. Laso, V. E. Boria, and M. Guglielmi, High-Performance Compact Diplexers for Ku/K-Band Satellite Applications, *IEEE Transactions on Microwave Theory and Techniques*, Vol.: PP, issue: 99, pp. 1 – 11, 2017.

[16] A. C. Das and S. Dwari, Analysis of Field Propagation through a Multiport Frequency Selective Network Using Cavity Modeling Technique, *Progress In Electromagnetics Research C*, vol. 82, pp. 209–223, 2018.

[17] A. C. Das, S. Dwari, and S. Priyadarsini Biswal, Applicability of Cavity Modeling Technique to Analyze Complex Waveguide Structures Involving Cavity Cross Couplings, *Wireless Personal Communications*, vol. 108. pp. 1431-1445, 2019.

[18] R. F. Harrington, *Time-Harmonic Electromagnetic Fields*, McGraw-Hill Book Company, New York, 1961.

[19] A. Vengadarajan., "Multiple Cavity Modelling Technique For Solving Aperture Coupled Waveguide Junctions," Ph.D. Dissertation, IIT Kharagpur, India 1999.

[20] R. F. Harrington, *Field Computation by Moment Methods*, Roger E. Krieger Publishing Company, USA.

Biography of the authors

Ashmi Chakraborty: Ashmi Chakraborty obtained her PhD Degree from Indian Institute of Technology (ISM) Dhanbad, India in 2019. She has worked as a Project Assistant at Indian Institute of Technology Kharagpur, India from 2003 to 2007. In 2007 she joined Asansol Engineering College, Asansol, India as a Lecturer, where she is now an Assistant Professor in the Department of Electronics and Communication Engineering. Her area of specialization is Microwave Networks.

Santanu Dwari: Santanu Dwari obtained his PhD degree from Indian Institute of Technology, Kharagpur, India in 2009. He joined Indian Institute of Technology (ISM), Dhanbad, India in 2008, where he is currently an Associate Professor in the Department of Electronics Engineering.He has published many research papers in reputed International Journals. His research interest includes Antennas and RF Circuits and Networks.

DOI: http://dx.doi.org/10.32452/IJAMT.2022.296300